SLAC-PUB-10820
October 2004

# Future GeV γ-ray Missions and New Discovery Potential

Tuneyoshi KAMAE

*Stanford Linear Accelerator Center and Kavli Inst. Part. Astro. Cosmology*
*Stanford university*

**Abstract.** Future GeV γ-ray missions, efforts to improve the diffuse γ-ray emission modeling, and possible exploitation of temporal variability for source characterization are reviewed. GLAST-LAT with its improved point-spread-function is expected to attain mCrab sensitivity, facilitate identification of γ-ray sources with those in other wavelength, and discover new source classes. However these new sources are likely to suffer from the Galactic diffuse background and/or the source confusion. Accurate modeling of the background will be essential to enhance discovery potential for Galactic sources and full exploitation of temporal variability will allow source identification even in highly confusing environment. GALPROP by Strong and Moskalenko provides a platform on which models and measurements on the cosmic ray, ISM and radiation field can be combined in a consistent way. An up-to-date high-energy *pp* interaction modeling has reduced the "GeV Excess" in the diffuse γ-ray spectrum significantly. Updating GALPROP with this interaction modeling as well as with other improvements will be needed before GLAST goes to orbit. The new temporal domain will be fully explored by GLAST-LAT as a new way to identify and characterize AGNs at cosmological distance.

## A FEW MILLI-CRAB SENSITIVITY FROM 100KEV TO 100TEV

Before the first decade of the 21st century closes, we will be able to map the entire sky in γ-ray from 100keV to 100TeV at sensitivity around a few to 10 milli-Crab. On the ground are 3 Air Cherenkov Telescopes (ACT: Cangaroo, HESS and Magic) operational, covering the highest 3 decades in the energy range above. Veritas is expected to join the three in 2005. In space is Integral covering the energy range from 100keV to 10MeV at a few to a few 100mCrab sensitivity. In a year Astro-E2 Hard X-ray Detector will join to cover between 10 and 500keV. The energy range from sub-GeV to hundreds of GeV will soon be covered by AGILE and GLAST-Large Area Telescope (LAT) of which GLAST-LAT will reach sensitivity around mCrab. The differential sensitivity of these instruments is plotted in Fig.1 together with popular multi-wavelength sources [1].

The instruments described above are or will be operated in the pointing mode except for GLAST whose observation time will be mostly in the survey mode. The observation times assumed in making the curves in Fig.1 are: 100ks (3σ) for Astro-E2 HXD; 1Ms (3σ) for Integral IBIS (ISGRI and PICsIT); 50hrs (5σ) for ACT's; 1Ms (5σ) for AGILE; 1 yr (5σ) for GLAST-LAT. EGRET sensitivity (3σ) has been calculated by the author on the paper by de Jager et al. of the Crab nebula (total 300hrs) [2]. The AGILE and GLAST sensitivities are based on Monte Carlo simulation and to be considered as preliminary. The source fluxes shown in Fig.1 have been calculated on observational data except for Cas A where a model prediction has been used to interpolate between hard X-ray observations and a TeV γ-ray

Work supported in part by the Department of Energy Contract DE-AC02-76SF00515

Stanford Linear Accelerator Center, Stanford University, Stanford, CA 94309

Invited talk presented at Gamma 2004: International Symposium on High Energy Gamma-Ray Astronomy, 7/26/2004 - 7/30/2004, Heidelberg, Germany

observation [1]. We note that there is a gap in the sensitivity coverage between 0.5MeV to 20MeV.

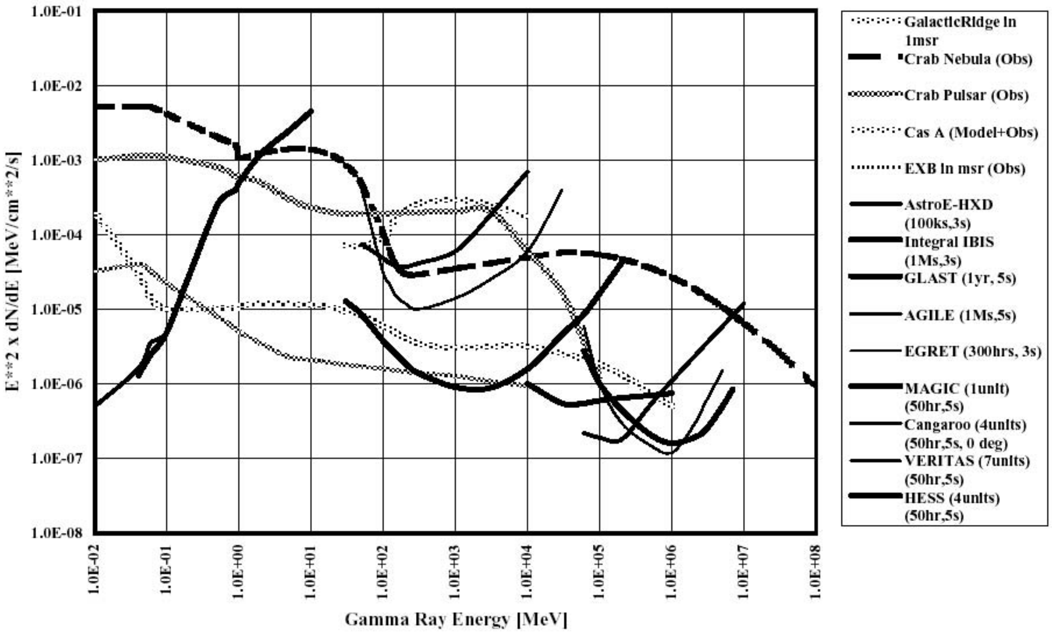


**FIGURE 1.** Differential sensitivities of instruments (from left to right): AstroE2-HXD (medium-thick solid: 100ks, 3σ), Integral-IBIS (thick solid: 1Ms,3σ), EGRET (thin solid: 300h, 3σ), AGILE (medium-thick solid: 1Ms, 5σ), GLAST-LAT (thick solid: 1yr, 5σ), Magic (thick solid: 50h, 5σ), Cangaroo (medium-thick solid: 50h, 5σ), Veritas (thin solid: 50h, 5σ), and HESS (thick solid: 50h, 5σ). Reference source spectra are (from high to low flux at 1GeV): Galactic Ridge (light-density band); Crab Pulsar (high-density band), Crab Nebula (thick dash), Cas A (light-density band), and Extra-Galactic Background in 1msr (medium-density band). References are given in [1].

## GLAST: High Sensitivity All Sky Gamma-Ray Monitor

GLAST-Large Area Telescope [3] is expected to bring the γ-ray astronomy to a new level by its unprecedented sensitivity. New categories of γ-ray sources are likely to emerge from a few thousands of point sources LAT will detect. Nearly 100 GRBs will occur in its wide field-of-view (FOV: about 2.5sr), every year, of which it will record sub-GeV to GeV γ-rays in the prompt burst, the delayed emission, and/or the after-glow. GLAST-LAT will most likely detect AGN flares before any other instruments and alert them of the events. Its extended spectral coverage from 20MeV to 300GeV and finer spatial resolution will map out the baryonic mass distribution with an angular resolution comparable to modern large-area CO surveys of the Galaxy, SMC, and LMC. Cosmic ray interaction with ISM and radiation in M31 and near-by galaxy clusters will also be detected for the first time. Its unprecedented wide field-of-view (about 2.5sr) will give reasonably uniform sky coverage every orbit (about 90 minutes) as shown in the left panel of Fig.2. The daily coverage in the survey mode will be both deep and uniform as shown in the right panel: all variability at 30-100 mCrab level will be detected on daily basis [3].

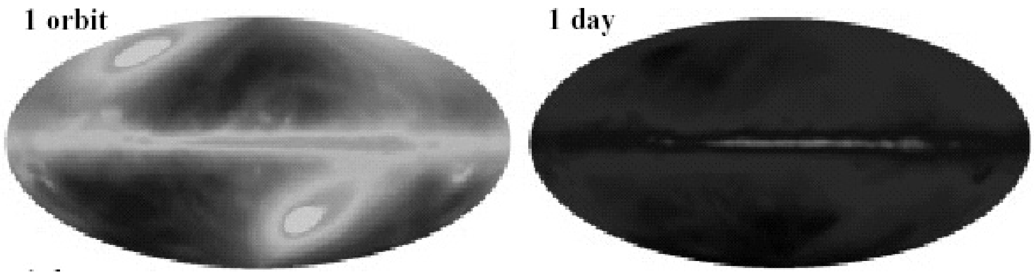


**FIGURE 2.** Sensitivity reach of GLAST-LAT in the Galactic coordinate is shown for one 90 minute orbit (left panel) and for a typical day (right panel). Sensitivity increases with darkness in the plots.

GLAST-LAT has about 75m$^2$ of silicon strip detectors to track the $e^+e^-$ pair created by a γ-ray. Its point-spread-function (PSF) is significantly narrower than that of EGRET, especially above 500MeV [3]. For a hard γ-ray source such as RXJ1713.7-3946, GLAST-LAT will give angular resolution comparable to that obtained by HESS in the stereo view operation [4] (see Fig.3).

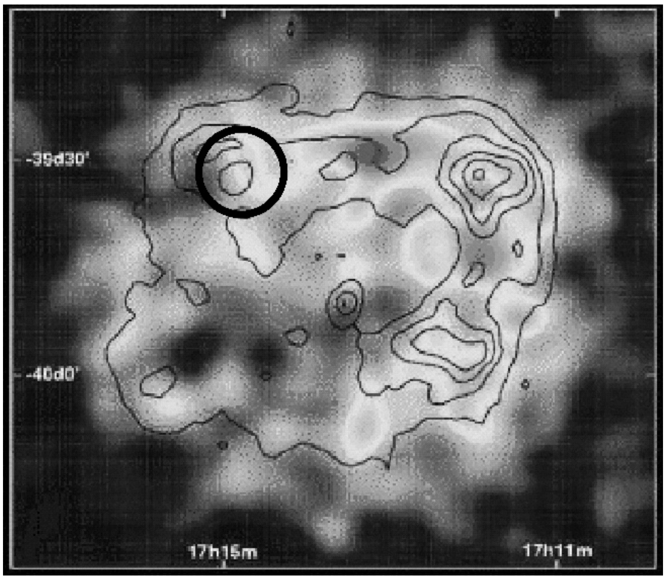


**FIGURE 3.** Point-spread-function (68% containment) of GLAST-LAT per 10GeV γ-ray (the black ring) superimposed to the γ-ray map of SNR RXJ1713.7-3946 obtained by HESS (gray scale map) [4].

Another strength of GLAST-LAT is its temporal resolution. The absolute timing accuracy will be determined by on-board GPS while the dead time by the trigger logic to be about 25μs. Hence GLAST-LAT can reveal timing structure down to about 50μs and can record densely packed γ-rays in bursts at a high efficiency [3].

## ANALYSES ON EGRET UN-ID'ED POINT SOURCES

EGRET has detected about 270 point-like sources but failed to identify even high flux GeV sources with sources recorded in other wavelength [5]. Efforts to identify them have been reviewed by Reimer in these proceedings [6]. We have sorted the un-identified sources in the descending order of the predicted GeV flux ($E_\gamma$>1GeV) for GLAST-LAT and listed their possible counter parts in Table 1 [7]. Certainty of the proposed identifications are not easy to assess but γ-ray pulsars appear to make up a large fraction. Even with dedicated observations in the X-ray and radio bands, most high flux sources remain not identified with certainty because of source confusion.

**Table 1. EGRET UnID Sources Sorted by Expected >GeV Flux for GLAST-LAT**

| Catalog No. | Glon | Glat | Possible ID | References [7] |
|---|---|---|---|---|
| 3EG_J1835+5918 | 88.74 | 25.07 | γ-ray pulsar | Mirabal et al. 01 |
| 3EG_J0852-1216 | 239.06 | 19.99 | | |
| 3EG_J2021+3716 | 78.06 | 0.33 | γ-ray pulsar | Roberts et al. 02 |
| 3EG_J2033+4118 | 80.27 | 0.73 | OB assoc ? | Benaglia et al. 01 |
| 3EG_J1856+0114 | 34.6 | -0.54 | PWN or SNR? | Roberts et al. 04 |
| 3EG_J1837-0606 | 25.86 | 0.4 | New class? | Tavani et al. 97 |
| 3EG_J1027-5817 | 284.94 | -0.52 | | |
| 3EG_J0010+7309 | 119.92 | 10.54 | PWN or Pulsar? | Mukherjee et al. 04 |
| 3EG_J1048-5840 | 287.53 | 0.47 | PSR B1046-58 | Kaspi et al., 00 |
| 3EG_J0617+2238 | 287.53 | 0.47 | IC 443? | Hnatyk et al. 98<br>Roberts et al. 01 |
| 3EG_J1826-1302 | 18.47 | -0.44 | PWN? | Roberts et al. 01,04 |
| 3EG_J1958+2909 | 66.23 | -0.16 | | |
| 3EG_J0241+6103 | 135.87 | 0.99 | | |
| 3EG_J1410-6147 | 312.18 | -0.35 | SNR G312.4-0.2? | Doherty et al. 03 |
| 3EG_J1800-2338 | 6.25 | -0.18 | PSR B1758-23? and/or W28? | Roberts et al. 01 |
| 3EG_J1734-3232 | 355.64 | 0.15 | | |
| 3EG_J1744-3011 | 22.19 | 13.42 | | |
| 3EG_J1420-6038 | 313.63 | 0.37 | γ-ray pulsar? and/or<br>Rabbit PWN? | Roberts et al. 01<br>Roberts et al. 99 |
| 3EG_J1625-2955 | 348.67 | 13.38 | | |
| 3EG_J0530+1323 | 191.5 | -11.09 | | |

## ANALYSES OF GALACTIC DIFFUSE GAMMA-RAY EMISSION

The spectrum and spatial distribution of the diffuse Galactic γ-ray emission by EGRET have induced many papers and discussions since early 1990s. In particular, inability to reproduce the observed Galactic diffuse γ-ray spectrum by conventional *pp* interaction models led to a possible anomaly known as the "GeV Excess" [8]. Another important progress in this area is establishment of the strong inverse Compton component in the Galaxy [9].

Strong, Moskalenko, and Reimer have updated their diffuse Galactic γ-ray modeling with the new version of GALPROP and with up-to-date CO, HI and interstellar radiation field (ISRF) measurements [10]. Fig.4 shows their results for $E_\gamma$=100-150MeV (left panel) and 150-300MeV (right panel). The upper solid curves represent the prediction with the conventional parameter set, which reproduces the shape of the EGRET distribution (points with error bars) reasonably well. The model, however, over-predicts the absolute magnitude especially in the negative longitude region [10]. At higher energy bands (not shown here), the model agrees with the data in the negative longitude region but falls short of the data in the Galactic central region [10]. A new analysis on GALPROP has been presented recently with a different cosmic ray source distribution, where the agreement in the longitudinal distribution has been improved further [11].

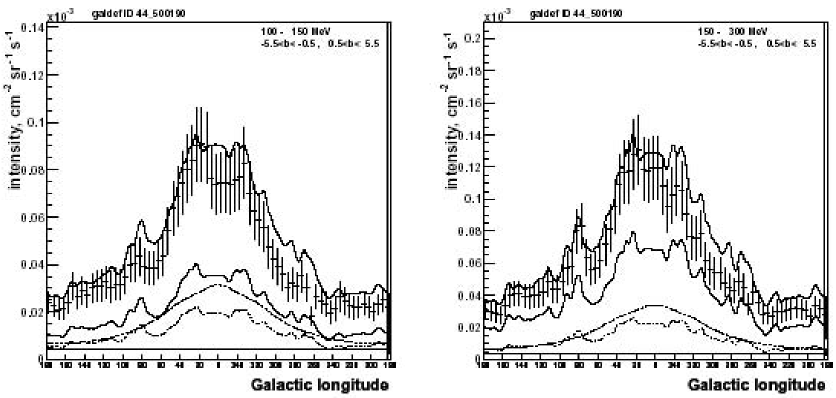


**FIGURE 4.** Diffuse γ-ray intensity (integrated over |*b*|<5 degree) along Galactic longitude for $E_\gamma$=100-150MeV (left panel) and $E_\gamma$=150-300MeV (right panel): Data points: EGRET, upper solid curve: sum of all components, lower solid curve: $\pi^0$ contribution, smooth dot-dot-dash curve: inverse Compton contribution, and lower dot-dash curve: bremsstrahlung contribution. [10].

One comment is in order here regarding the Galactic diffuse γ-ray distribution. The traditional way of studying the Galactic diffuse γ-ray distribution has been to compare the EGRET observation with PSF-smeared model predictions. The EGRET data used in the study of Galactic diffuse emission were taken in the pointed observation centered at around the Galactic center or on the Galactic plane. The angular extent of the emission along the Galactic latitude (*b*) is similar to the spread of the instrument PSF at lower energy bands ($E_\gamma$<300MeV). Under such circumstance, on-axis low-energy γ-rays scattered by a large angle (comparable to the spread in the PSF) are normalized by the exposure estimated for the scattered direction, which is significantly smaller than that of on-axis. This causes significant systematic spill over from the Galactic ridge (eg. |*b*|<2 degree) to higher latitudes (eg. |*b*|>2) in a manner not reproducible by convolving theoretical predictions with the PSF. Because of this bias,

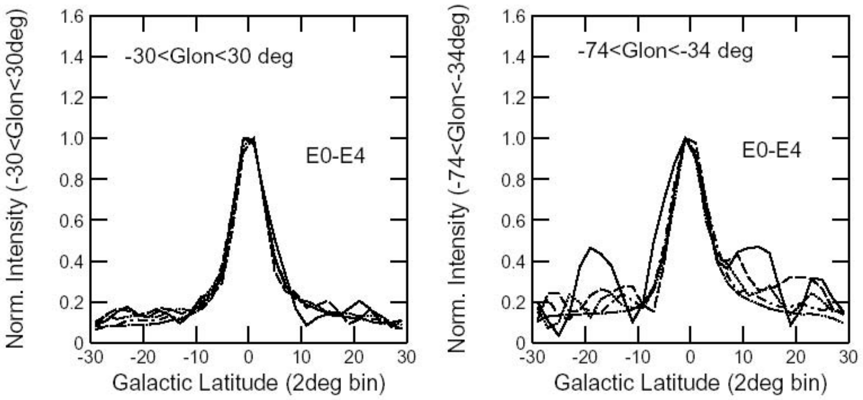


**FIGURE 5.** PSF-deconvolved diffuse γ-ray intensity distribution of EGRET along the Galactic latitude in the Galactic longitude region between –30 and 30 degree (left panel) and –74 and –34 degree (right panel). The 5 curves are for E=30-50MeV (solid), 50-70 (dash), 70-100 (dot), 100-150 (dot-dash), and 150-300 (dot-dot-dash) [12].

the author and coworkers has de-convolved the point-source-subtracted count before dividing (ie. normalizing) with the exposure [12]. Fig.5 shows the Galactic latitude distribution in the longitude regions between –30 and 30 degree (left panel) and between –74 and –34 degree (right panel). We see in both panels, that Gaussian-like distributions centered at the Galactic plane (*b*=0) overlap for all 5 energy bands, from 30 to 300MeV. This overlap confirms, model independently, that the dominant emission mechanism is tied to the matter distribution [12]. Note that the solid curve representing the lowest energy band (E=30-50MeV) consists of very few photons: about 20 γ-rays in the 2x2 degree pixel at the Galactic center and a few or less off the Galactic plane. We also note that there is no room for a high flux yet-to-be discovered point source (eg. >100mCrab) in the Galactic ridge.

## ACCURATE MODEL OF *PP* INTERACTION

The author and coworkers found that $pp \rightarrow \pi^0$ models used in the past to predict the Galactic γ-ray spectrum [13] need the following 3 important upgrades:

1) Include the diffractive process;
2) Use the up-to-date non-diffractive ineleastic cross-section;
3) Incorporate the Feynman scaling violation.

The up-to-date inelastic cross-sections (non-diffractive and diffractive) shown in the left panel (Model A) of Fig.6 can be compared with a typical inelastic cross-section (non-diffractive) used until now (shown in the right panel labeled as Model B) [14].

The new *pp* interaction model for cosmic-ray interaction proposed includes the diffractive interaction, incorporates the Feynman scaling violation and uses the accurate inelastic cross-sections for the first time [14]. The combination of the three predicts more γ-rays at higher energies (Model A in the left panel of Fig.7) than the old modeling without scaling violation (Model B in Fig.7 left panel). The diffraction process adds γ-rays at the highest and lowest ends of the γ-ray spectrum (Fig.7 right panel). These 2 effects produce more γ-rays in the GeV range and make the γ-ray spectrum harder than the incident proton spectrum by about 0.05 in power-law index (Fig.8). Assuming for the cosmic ray spectrum, the local interstellar spectrum (LIS), the new interaction model predicts the $\nu f(\nu)$ γ-ray spectrum to peak at around 0.8 GeV, closer to that of EGRET data as shown in the left panel of Fig.9.

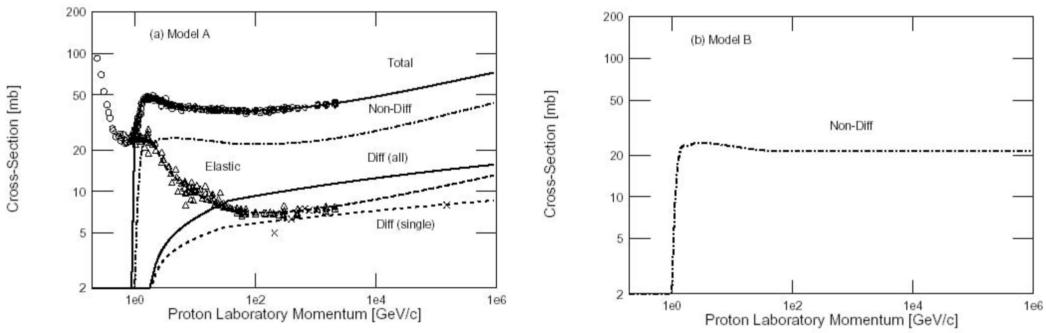


**FIGURE 6.** Up-to-date *pp* interaction cross-sections (left panel) and a typical cross-section used in predicting $\pi^0$ γ-ray spectrum in the past (right panel). The ones label as Non-Diff, Diff(single) and Diff(all) in the left panel have been used in the new model (Model A) described in the text. From [14].

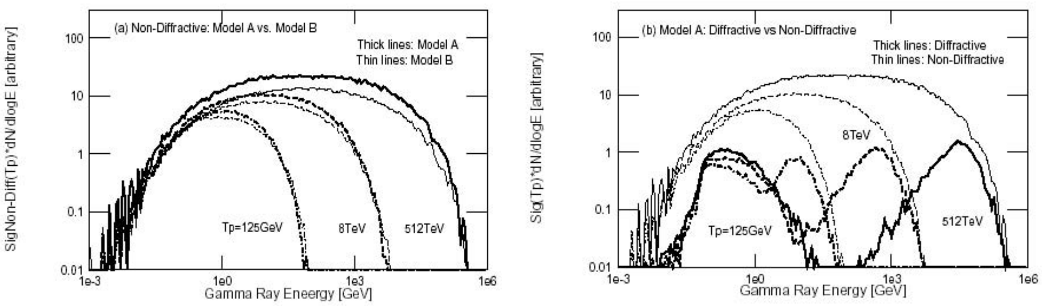


**FIGURE 7.** Left panel: Comparison between the inclusive $\pi^0$ γ-ray spectra of the new model (Model A, thick curves) and that of a typical old model (Model B, thin curves) for proton energies of 125GeV, 8TeV and 512TeV. Right panel: Comparison between the non-diffractive (thin curves) and diffractive (thick curves) $\pi^0$ γ-ray spectra for the 3 proton energies. From [14].

Besides protons, cosmic ray electrons produce high-energy γ-rays through bremsstrahlung and inverse Compton. The bremsstrahlung and inverse Compton spectra calculated by Strong, Moskalenko and Reimer [10] have been combined with the γ-ray spectrum predicted by the new $pp \rightarrow \pi^0$ model to obtain the total γ-ray spectrum, the dashed line labeled as Model A with LIS in the right panel of Fig.9. There, the "GeV Excess" is reduced to about a half without introducing new particles nor drastically changing any cosmic-ray spectrum. If the proton spectrum is a little

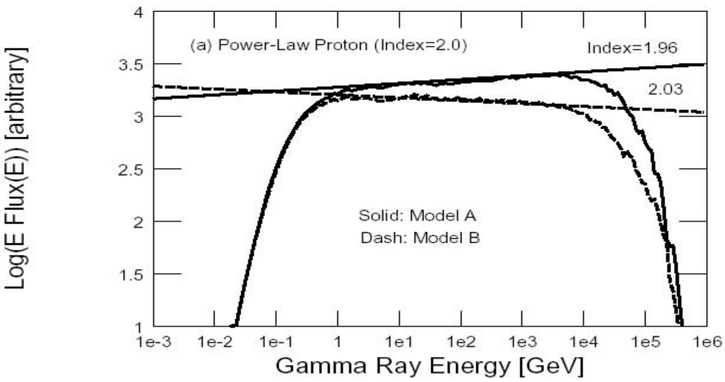


**FIGURE 8.** Gamma-ray spectra produced by power-law protons (index=2.0, 0.488GeV<$T_p$<512TeV): predictions by the new model (Model A, solid curve) and a typical old model (Model B, dashed curve). Note that the asymptotic power-law index for Model A is higher than Model B by 0.07. From [14]

harder (by 0.2 in power-law index) in the Galactic ridge than in the solar neighborhood, the new *pp* interaction model will predict the solid line (labeled as Trial4GR) in the right panel of Fig.9. The "GeV Excess" is then fully explained.

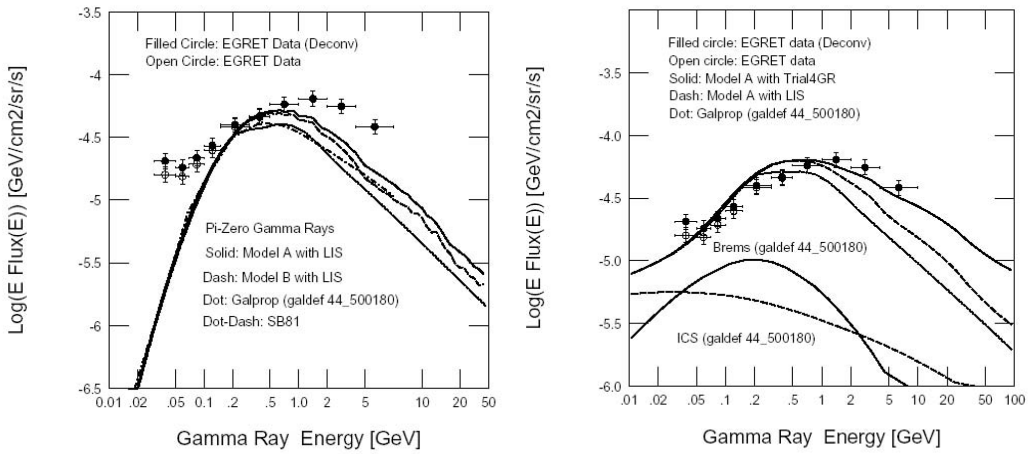


**FIGURE 9.** Left panel: Gamma-ray spectra from $\pi^0$ decay predicted by the new model (Model A) with LIS [14], a typical old model (Model B) with LIS, the GALPROP modeling with LIS (Galprop) [10], and, Stephen and Badhwar (SW81) [13]. Right panel: Total Galactic diffuse γ-ray spectra predicted by the new model (Model A) with LIS and a harder-than-LIS spectrum, and the GALPROP modeling with LIS [10]. Data are the PSF deconvolved spectrum (open circle [12]) and or raw spectrum (filled circle) in the Galactic region (-30<*l*<30 deg, -6<*b*<6 deg). The error bars represent the assumed systematic error of 15%.

In addition to making the γ-ray spectrum harder, the new model of pp interaction changes the secondary $e^+$, $e^-$, neutrino and p-bar spectra significantly [14]. For example, the diffractive interaction produces 20-30% more $e^+$ than $e^-$ in the high energy end of the $pp \rightarrow \pi \rightarrow$ electron spectrum as shown in Fig.10. The up-to-date non-diffractive inelastic cross-section and scaling violation make 50-100% more p-bar in the GeV range than a typical old model (Model B) as shown in Fig.11.

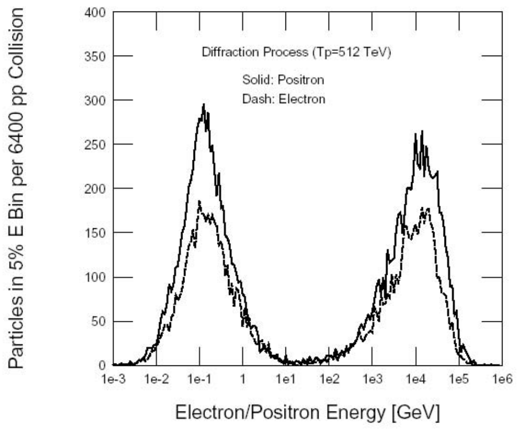


**FIGURE 10.** Spectra of electrons (dash) and positrons (solid) produced in 6400 diffractive interactions by protons with $T_p$=512TeV. From [14].

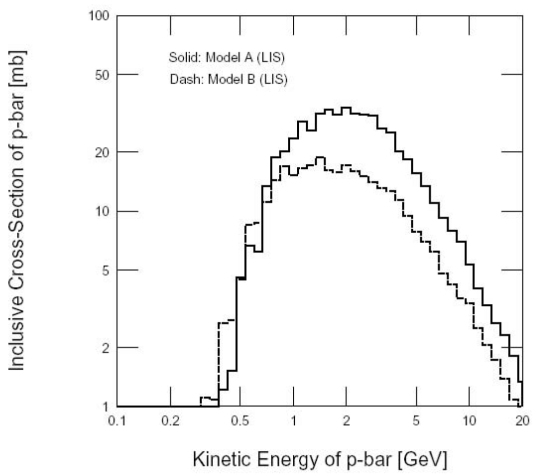


**FIGURE 11.** Anti-protons spectra predicted for the local cosmic ray proton spectrum (LIS) by the new model (Model A, solid) and by a typical old model (Model B, dash). The bin width is 5% of proton kinetic energy. From [14].

## UNEXPLORED TEMPORAL DOMAIN

Until recently, X-ray instruments lagged behind optical telescopes in the spatial and spectral resolutions. With Chandra and XMM, X-ray astronomy has finally caught up with optical astronomy in these capabilities. With the micro-calorimeter on board AstroE2, X-ray astronomers will be endowed with instantaneous high spatial and spectral resolution for the first time in astronomy [15]. In the shorter end of temporal domain, however, the slow temporal response of the X-ray CCD and micro-calorimeter has been limiting study on kHz QPO and possible structure in the narrow pulse profile of some millisecond pulsars. The silicon trackers used in AGILE and GLAST-LAT as well as phototubes used in the atmospheric Cherenkov telescope will enable to study temporal variability down to microsecond range. In the longer end of temporal variability, the capability to monitor daily over many years of GLAST-LAT will open a new genre in astronomy. In this section, a few related topics will be discussed.

## Source Identification Based on Longer-Term Variability

Short-term variability has long been applied in characterizing sources in the radio, optical and X-ray bands. Less explored is the long-term variability. EGRET team members and others have applied this method to EGRET data [16] and brought success in reducing possible candidates [7]. EGRET was operated in the pointing mode and temporal sampling was limited and sparse. GLAST-LAT will monitor systematically the entire sky every day over 5-10 years. This systematical recording of long-term variability for all sources can become a powerful method to identify γ-ray sources, should similar long-term deep monitoring become available in other wavebands, eg. in X-ray [17].

## Pulsar Stability Including Glitches

Traditionally, instability including glitches in radio pulsars has been monitored in the radio band [18]. In near future, gamma-loud radio-quiet pulsars will also be monitored by GLAST-LAT. One exciting possibility GLAST-LAT will bring with its wide FOV is to record the very moment when a glitch occurs.

## Lensing in Time Domain

Another exciting possibility with GLAST-LAT is detection of gravitational lensing in the time domain. Several authors have studied possible micro-lensing where γ-ray intensity gets enhanced in a well predicted way over several days [19]. Because of the systematic surveying of GLAST-LAT over many years, we will also observe several strong lensing events in the temporal coordinate where a similar light curve (eg. a flare) will be repeated several months apart like many such recurrences found in the radio band [20]. Lensing will allow us to identify GLAST-LAT sources at cosmological distance with counter parts observed by VLA. Comparison between the γ-ray and radio bands will characterize the sources and bring important cosmological information.

## CONCLUSION AND FUTURE PROSPECTS

With the new γ-ray observatories reviewed here and in the workshop, we will obtain mCrab sensitivity from 100keV to a few TeV and open up enormous discovery potential. The new discovery potential will be limited in the Galactic bulge and halo (for example $|b|<20$ deg) unless we come up with much improved modeling of Galactic diffuse emission mechanism. In the high Galactic latitude, the source confusion has been the major hurdle for source identification. Even with the improved PSF of AGILE and GLAST-LAT, this limitation will remain at a lower flux level.

GALPROP provides a platform on which models and measurements on the cosmic ray, ISM and radiation field can be combined in a consistent way. A new accurate modeling of proton-ISM interaction has shown that the "GeV Excess" of EGRET is reduced to about a half. This interaction modeling needs to be incorporated to GALPROP, and, various parameters in GALPROP has to be re-optimized. Such improvement will enhance predictability of the diffuse γ-ray emission and enhance discovery potential in this region.

GLAST-LAT is capable of exploring the new temporal domain in full and establishing a new way to identify or characterize low flux sources even if several potential sources are within the source confusion limit. What is highly desired is similar deep monitoring instrument in other waveband, eg. the X-ray and radio bands. MAXI [17] offers such possibility in the X-ray band.

## ACKNOWLEDGMENTS

The author would like to acknowledge valuable guidance given by I. Moskalenko, A. Strong, O. Reimer, M. Roberts, D. Torres, D. Soward-Emmerd, T. Abe, T. Koi, and K. Goulianos. He also wishes to acknowledge assistance given by D. Elwe, J. Chiang, S. Digel, G. Madejski, H. Tajima, P. Nolan, R. Hartman, S. Hunter, M. Mori, J. Ormes, F. Stecker, D. Thompson, M. Asai, N. Graf and Y. Shimizu.

## REFERENCES

1. Sensitivity curves are produced on data obtained either from the official web sites or conference presentations on the instrument or from the instrument headquarter. Atmospheric Cherenkov Telescopes traditionally use sensitivity for flux above E. The differential sensitivity curves given here has been calculated assuming a Crab-like spectrum. Note most curves are read out by eye of plots given below and can be off by 20-30%.
   - AstroE2-HXD (SiPIN+GSO): H. Soojing http://eaya2003.asiaa.sinica.edu.tw/pdf/hong_sj.pdf,
   - Integral IBIS (ISGRI+PICsIT): R. Diehl, "Integral Overview" Magic Physics 2002 Workshop,
   - GLAST-LAT: http://www-glast.slac.stanford.edu/software/IS/glast_lat_performance.htm
   - AGILE: http://agile.mi.iasf.cnr.it/Homepage/performances.shtml
   - EGRET: Since there is no official sensitivity curve available, the author calculated based on the Crab observation (see the text). So admittedly not official and may lack accuracy.

- Magic: http://hegra1.mppmu.mpg.de/MAGICWeb
- Cangaroo: http://icrhp9.icrr.u-tokyo.ac.jp/paper/C3.pdf (in Japanese)
- HESS: http://www.mpi-hd.mpg.de/hfm/HESS/HESS.html
- Veritas: http://veritas.sao.arizona.edu/

The spectra of popular sources have been interpolated if experimental data are sparse or missing in a large portion of spectrum. Hence they are to be taken as crude references.

- Crab Nebula and Pulsar: de Jager [2]; Kuiper, L., et al., 2001, A&A 378, 918; Nolan, P. L., et al., 1993, ApJ 409, 697
- Cas A: Favata, F., et al., 1997, A&A 324, L49; Aharonian, F., et al., 2001, A&A 370,112; Atoyan, A. M., et al., 2000, A&A 355, 211
- Extragalactic Background (EXB): Sreekumar, P., et al., 1998, ApJ 494, 523

2. de Jager, O. C., et al., 1996, ApJ, 457, 253
3. GLAST-LAT official website, http://www-glast.stanford.edu/
4 Hofmann, W., these proceedings
5. Hartmann, R. C., et al., 1999, ApJ Suppl. 123, 79
6. Reimer, O., these proceddings
7. Reviews in http://www.physics.hku.hk/~2003conf/participants.html
   (Benaglia et al. 01) Benaglia, P., et al., 2001, A&A 366, 605
   (Hnatyk et al. 98) Hnatyk, B., and Petruk, O., 1998, Condensed Matter Physics Vol.1, 655
   (Kaspi et al. 00) Kaspi, V. M., et al., 2000, ApJ 528, 445
   (Mirabal et al 01) Mirabal, N., and Halpern, J. P., 2001, ApJ 547, L137; Halpern, J. P., et al., 2002 ApJ 573, L41
   (Mukerjee et al 04) Mukherjee, R., and Halpern, J., 2004, astro-ph/0408063
   (Roberts et al. 99) Roberts, M. S. E., et al., 1999, ApJ 515, 712
   (Roberts et al. 01) Roberts, M., Romani, R. W., and Kawai, N., 2001, ApJ Suppl. 133, 451
   (Roberts et al. 02) Roberts, M. S. E., et al., 2002, ApJ 577, L19
   (Roberts et al. 04) http://www.physics.hku.hk/~2003conf/participants.html and astro-ph/0409104
8. Hunter, S. D., et al., 1997, ApJ 481, 205
9. Schlickeiser, R., 1979, ApJ 233, 294; Chen, A., Dwyer, J., and Kaaret, P., 1996, ApJ 463, 169; Strong, A., Moskalenko, I., and Reimer, O., 2000, ApJ 537, 763
10. Strong, A., Moskalenko, I., and Reimer, O., 2004, ApJ 613, 962
11. Strong, A., Moskalenko, I., Reimer, O., Digel, S., and Diehl, R., 2004, A&A 422, L47
12. Kamae, T., et al., in preparation
13. Stephens, S.A., and Badhwar, G.D., 1981, Astrophys. Space Sci, 76, 213;
    Dermer, C. D. 1986, A&A, 157, 223
    Stecker, F. 1989, in Shapiro, M.M., and Wefel, J.P. (eds.), ``Cosmic Gamma Rays, Neutrinos and Related Astrophysics", p.89
    Mori, M., 1997, ApJ, 478, 225
    Also the neutral pion production simulation in GALPROP.
14. Kamae, T., Abe, T., and Koi, T., ApJ (accepted)
15. Astro E2 XRS Team, http://phonon.gsfc.nasa.gov/xrscal/SHI2004/index.html
16. Thompson, D. J., 2001, AIP vol.558, p.103
    Nolan, P. L., Tompkins, W. F., Grenier, I. A., and Michelson, P. F., 2003, ApJ 597, 615
    Torres, D. F., et al., 2003, Physics Reports, 382(6), 303
    Soward-Emmerd, D., et al., 2004, ApJ 609, 564
17. MAXI may provide such a possibility: http://www-maxi.tksc.nasda.go.jp/indexe.html
18. See for example, Wang, N. et al., 2000, MNRS 317, 843 (southern sky pulsars) and
    Cognard, I., and Backer, D. C., astro-ph/0407546 (a milli-second pulsar)
19. Wyithe, S., and Turner, E. L., 2002, ApJ 567, 18
    Torres, D. F., Romero, G. E., and Eiroa, E. F., 2002, ApJ 569, 600
20. Falco, E. E., Kochanek, C. S., and Munoz, J. A., 1998, ApJ 494, 47
    See also a cosmological analysis on them in: Cooray, A. R., 1999, A&A 342, 353